COMMUNICATION

Check for updates

Ruthenium(II)-catalyzed C-2 alkenylation of indole with olefins *via* a quinazolin-4(3H)-one directing group: a platform for selective fluorescent anion sensors

Rekha Thakur, Vijay Luxami [ID] and Kamaldeep Paul [ID]*

We report a ruthenium(II)-catalyzed C−H alkenylation of 2-(1*H*-indol-3-yl)quinazolin-4(3*H*)-one with various alkenes. The reaction proceeds selectively at the C2 position of the indole moiety, facilitated by a cyclic amide as the directing group. Furthermore, the synthesized compounds were evaluated for their photophysical properties, revealing intriguing fluorescence characteristics that highlight their potential as promising fluorescent probes.

As one of the most privileged heterocycles, indole scaffolds have extensive applications in medicinal and materials chemistry.[1,2] Indole derivatives are found in numerous natural products and pharmaceuticals, and show a wide range of biological activities including anticancer, antimicrobial, anti-inflammatory, and antifungal properties.[3–5] Indole-based ligands can interact with metal centers, which are capable of binding with various receptors.[6,7] Direct C–H functionalization of indoles has emerged as a powerful and straightforward route to synthesize substituted indoles.[8] Transition metal-catalyzed C–H functionalization at different positions of indoles has been achieved by utilizing various directing groups.[9,10] The synthesis of C2-functionalized indoles has gained the interest of chemists because of their applications in medicinal chemistry.[11] Li and coworkers reported cobalt(III)-catalyzed C2-fluoroalkenylation of indoles using *N*-pyrimidine as a directing group (Scheme 1a).[12] Most of the carbonyl-based directing groups favor C4 C–H functionalization.[13] In 2017, Jia and coworkers reported Rh(III)-catalyzed C4-alkenylation of indole-3-carboxaldehyde using an aldehyde as a directing group (Scheme 1b).[14]

Different alkenylated agents such as activated alkenes or alkynes have been used so far to obtain alkenylated indoles using transition metal catalyzed C–H functionalization.[15] Wu and coworkers reported Rh(III)-catalyzed C2-alkenylation of indole using CF$_3$-imidoyl sulfoxonium ylides as alkenylating agents (Scheme 1c).[16] Despite significant progress in the C2-alkenylation of indoles, developing other structurally diverse directing groups is still highly important and desirable. To the best of our knowledge,

there are no reports on the selective C2-alkenylation of indoles using a cyclic amide as a directing group. With our continuous efforts to develop late-stage C–H functionalization strategies for biologically active molecules,[17] we herein report the Ru(II)-catalyzed C–H functionalization of indolyl quinazolinone with various alkenes (Scheme 1d). Here, this approach achieves selective C2-alkenylation of the indole moiety by employing a cyclic amide (quinazolin-4(3*H*)-one) as a directing group at the C3 position. Furthermore, the synthesized compounds are evaluated for their photophysical properties, leveraging their π-extended conjugation, and selective detection of F⁻ and CN⁻ ions.

We commenced our study by employing 2-(1*H*-indol-3-yl)quinazolin-4(3*H*)-one (**1a**) and methyl acrylate (**2a**) as substrates, [Ru(*p*-cymene)Cl$_2$]$_2$ as a catalyst, AgOAc as an oxidant, and AgSbF$_6$ as an additive in DMF under a nitrogen atmosphere at 120 °C. The product **3aa** was obtained in 40% yield (Table 1, entry 1). Next, we performed an extensive screening of the
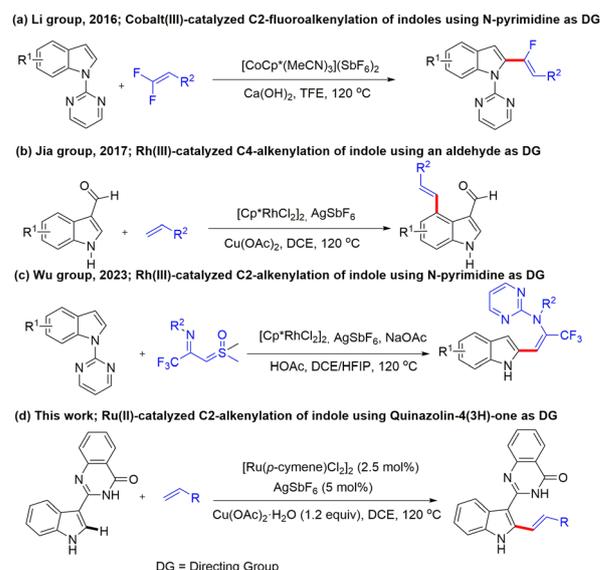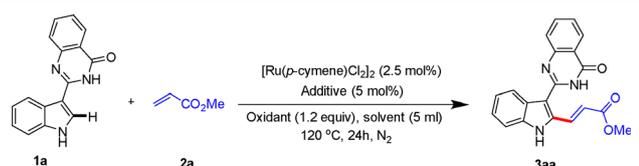

Scheme 1 Transition-metal catalyzed C−H alkenylation of indoles.

Department of Chemistry and Biochemistry, Thapar Institute of Engineering and Technology, Patiala, 147004, India. E-mail: Kpaul@thapar.edu

Table 1 Screening of the reaction conditions

Reaction conditions: **1a** (0.1 mmol), **2a** (0.15 mmol), [Ru(*p*-cymene)Cl$_2$]$_2$ (2.5 mol%), oxidant (1.2 equiv.), additive (5 mol%), solvent (1 mL), N$_2$, 120 °C, 24 h. ^{a} Isolated yields. ^{b} Pd(OAc)$_2$. ^{c} Pd(PPh$_3$)$_4$. ^{d} PdCl$_4$.

Entry	Oxidant	Additive	Solvent	Base	Yield^a (%)
1	AgOAc	AgSbF$_6$	DMF	—	40
2	AgOAc	AgSbF$_6$	DCE	—	60
3	AgOAc	AgSbF$_6$	THF	—	4
4	AgOAc	AgSbF$_6$	Dioxane	—	15
5	AgOAc	AgSbF$_6$	Toluene	—	Traces
6	AgOAc	AgSbF$_6$	NMP	—	20
7	Cu(OAc)$_2$·H$_2$O	AgSbF$_6$	DCE	—	82
8	Cu(OAc)$_2$·H$_2$O	AgSbF$_6$	DCE	KOAc	30
9	Cu(OAc)$_2$·H$_2$O	AgSbF$_6$	DCE	NaOAc	20
10	Cu(OAc)$_2$·H$_2$O	AgSbF$_6$	DCE	K$_2$CO$_3$	5
11	Cu(OAc)$_2$·H$_2$O	P(Cy)$_3$	DCE	—	Traces
12	Cu(OAc)$_2$·H$_2$O	AcOH	DCE	—	10
13	Cu(OAc)$_2$·H$_2$O	AdCO$_2$H	DCE	—	12
14^b	Cu(OAc)$_2$·H$_2$O	AgSbF$_6$	DCE	—	35
15^c	Cu(OAc)$_2$·H$_2$O	AgSbF$_6$	DCE	—	10
16^d	Cu(OAc)$_2$·H$_2$O	AgSbF$_6$	DCE	—	20

solvents. The yield of **3aa** was further improved to 60% when DCE was used as a solvent (Table 1, entry 2). Using the other screened solvents, such as THF, 1,4-dioxane, toluene, and NMP, gave inferior results (Table 1, entries 3–6). Furthermore, to increase the product yield, we screened various oxidants, such as CuO, Cu(OTf)$_2$, CuCl$_2$, Ag$_2$O, *etc.* (Table S2, SI), and all lowered the reaction yield. The yield of **3aa** was increased up to 82% in the presence of Cu(OAc)$_2$·H$_2$O (Table 1, entry 7). Adding bases, including KOAc, NaOAc, and K$_2$CO$_3$, decreased the reaction yield significantly (Table 1, entries 8–10).

The use of additives other than AgSbF$_6$ resulted in a low yield (Table 1, entries 11–13). However, the reaction without an oxidant gave only a sluggish product, indicating the importance of Cu(OAc)$_2$·H$_2$O. The reaction was also performed with palladium catalysts such as Pd(OAc)$_2$, Pd(PPh$_3$)$_4$ and PdCl$_4$, resulting in low conversion (Table 1, entries 14–16). With the optimized conditions in hands, we examined the scope of substituted indolylquinazolinones for this reaction (Scheme 2). The reaction was found to be compatible with substrates having indole moiety-bearing electron donating and electron withdrawing substituents to give the final products (**3ba–3ja**) in moderate to good yields (68–86%). Electron donating substituents such as Me (**3ba**) and OMe (**3ca**) at the C5 position of the indole moiety provided good yields of 86% and 83%, respectively. Substrates bearing halogens showed good tolerance and gave the products **3da–3ea** and **3ga–3ja** in good yields (68–76%). The position of the substituents on indole had no significant effect on the reaction yield, and substitutions at the C4, C5, and C6 positions were equally tolerated for the reaction. Delightfully, the reaction involving the substrate with *N*-methylindole, *N*-ethylindole, *N*-benzylindole, and *N*-allylindole proceeded efficiently resulting in
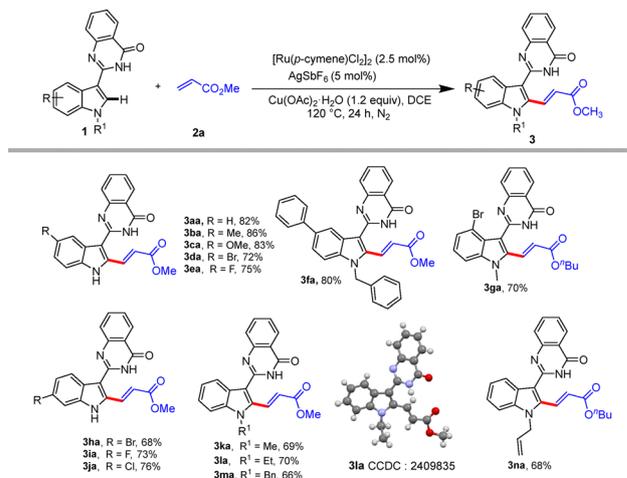

Scheme 2 Scope of the phenanthroimidazole substrate.^{a} Reaction conditions: **1** (0.38 mmol), **2a** (0.57 mmol), [Ru(*p*-cymene)Cl$_2$]$_2$ (2.5 mol%), Cu(OAc)$_2$·H$_2$O (1.2 equiv.), AgSbF$_6$ (5 mol%), DCE (2 mL), N$_2$, 120 °C, 24 h. ^{a} Yields of isolated products.

the desired products with satisfactory yields of **3ka** (69%), **3la** (70%), **3ma** (66%) and **3na** (68%), respectively.

Next, the scope of different alkenes towards this reaction was investigated. A variety of acrylates was compatible, giving the desired products in good yields (**3ab–3af**). The *tert*-butyl and isobornyl acrylate substituted compounds (**3ad** and **3af**) were produced in lower yields compared to others (Scheme 3), suggesting that steric hindrance significantly impacted these reactions. Other active alkenes like methyl vinyl ketone, styrene acrylonitrile, cyclohexenone, *etc.* were also examined.

Among these, acrylonitrile and styrene gave the desired products **3ag** and **3ah** in 65% and 62% yields, respectively. Other alkenes like methyl vinyl ketone and cyclohexenone were found to be unsuccessful.

Next, a gram-scale experiment was performed under the optimized reaction conditions at 3.8 mmol scale to demonstrate the synthetic utility of this reaction. The product **3aa** was obtained in 78% yield (Scheme 4).
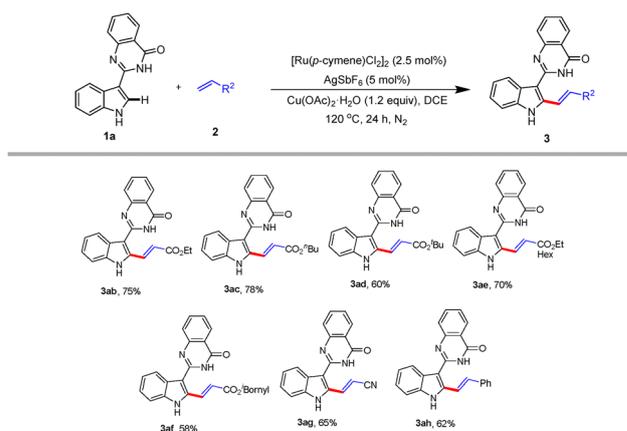
Scheme 3 Scope of alkenes.^{a} Reaction conditions: **1a** (0.38 mmol), **2** (0.57 mmol), [Ru(*p*-cymene)Cl$_2$]$_2$ (2.5 mol%), Cu(OAc)$_2$·H$_2$O (1.2 equiv.), AgSbF$_6$ (5 mol%), DCE (2 mL), N$_2$, 120 °C, 24 h. ^{a} Yields of isolated products.
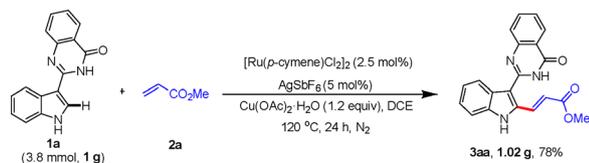
Scheme 4 Gram scale synthesis.

To get an insight into the reaction mechanism, preliminary control experiments were carried out. The reaction between 3-methyl indole and methyl acrylate did not give any alkenylated product, confirming the role of quinazolinone as a directing group (Scheme 5a). Furthermore, a series of deuterium labeling experiments were performed. The H/D exchange experiment of **1a** with D_2O without the addition of alkene gave **1a-[D]** with 50% deuteration at the C2 position of the indole ring (Scheme 5b).

On the other hand, reaction of **1a** with methyl acrylate in the presence of D_2O gave the product **3aa-[D]** with 40% deuteration at C2 of the indole moiety, indicating that the C–H activation step is reversible (Scheme 5c).[18] In addition, the kinetic isotope effect was determined by the parallel reaction with **1a/1a-[D]** to give $P_H/P_D = 1.05$, which indicates that C–H activation might not be the rate determining step (Scheme 5d).[19] Based on these experiments and previous literature reports,[20] we proposed the following reaction mechanism (Scheme 6). Initially, active catalyst [Ru(p-cymene)(OAc)]SbF₆ was generated from [Ru(p-cymene)Cl₂]₂ in the presence of Cu(OAc)₂ and AgSbF₆. Coordination of the quinazolinone nitrogen atom of substrate **1a** with the active catalyst followed by agostic interaction (**Int A-B**) and *ortho*-metalation provided an intermediate **B**. Alkene **2a** coordinated to the ruthenium center by substitution of the acetic acid ligand to give intermediate **C** that underwent
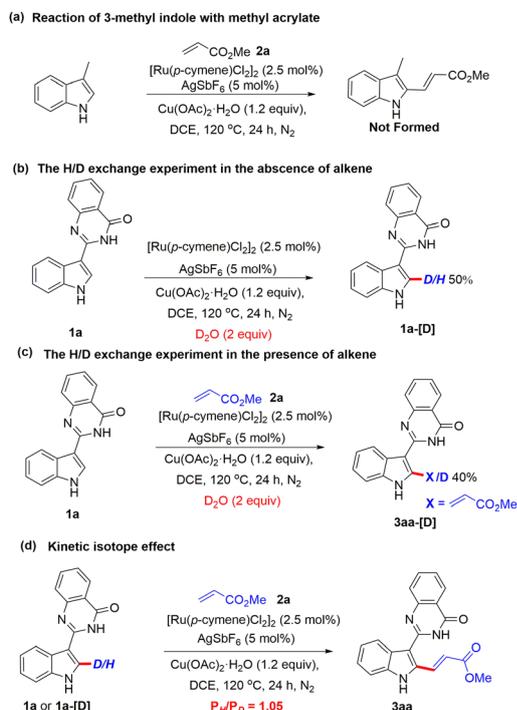

Scheme 5 Mechanistic experiments.
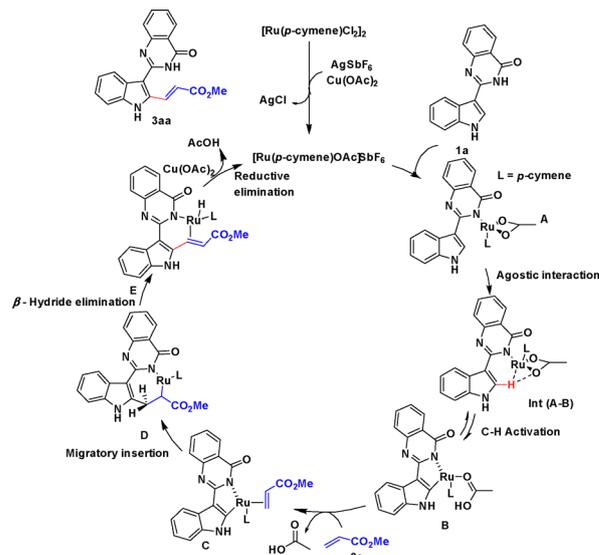
Scheme 6 Proposed mechanism.

migratory insertion to give intermediate **D**. β-Hydride elimination of **D** followed by reductive elimination afforded the alkenylated product **3aa**.

Photophysical properties. The extended conjugated systems in these molecules endowed them with potential to exhibit promising fluorescence properties.[21] Hence, we studied the photophysical behaviour of these alkenylated compounds. The absorption and emission spectra of compound **3** were recorded in CH_3CN at a concentration of 5×10^{-6} M (Table S8, SI). The absorption maximum of unsubstituted compound **3aa** appeared at 343 nm. Both electron-donating and electron-withdrawing substituents caused a bathochromic shift in absorption maxima, which ranged from 344 to 355 nm. Similarly, the emission maximum of compound **3aa** appeared at 525 nm with a Stokes shift of 9940 cm⁻¹. Substitution with an electron-donating methyl group (**3ba**) shifted the emission band to 535 nm with a Stokes shift of 9500 cm⁻¹. The bromo-substituted compound **3da** exhibited an emission maximum at 518 nm with a Stokes shift of 9765 cm⁻¹. Meanwhile, the phenyl substituted compound (**3fa**) showed an emission maximum at 545 nm with a Stokes shift of 10 640 cm⁻¹. Thus, the electron-donating substituents induce a bathochromic shift in the emission band, while in the case of electron-withdrawing substituents, the emission maxima showed a hypsochromic shift (Fig. 1a). Substrates with an electron-donating group showed an increase in fluorescence quantum yield (Φ_F) of 0.80 compared to those with an electron-withdrawing substituent ($\Phi_F = 0.66$). Interestingly, the introduction of an aromatic ring increased the quantum yield to a maximum of 0.88. Additionally, under UV light, compounds **3ba** and **3fa** also exhibited notable emission colour changes to mild blue and green fluorescence, respectively (Fig. 1b).

Next, we performed solvatochromic studies on the compound **3fa** due to its red shifted emission. The absorption maxima in various solvents showed minimal variation, ranging from 344 to 350 nm. On the other hand, the emission maxima were significantly affected by solvent polarity, shifting from 473 nm in methanol (polar solvent, Stokes shift = 7760 cm⁻¹,
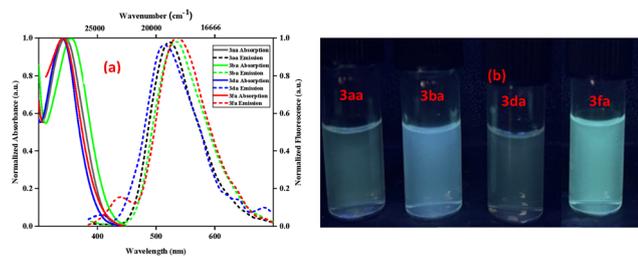
Fig. 1 (a) Absorption maxima (solid lines) and emission maxima (dashed lines), and (b) under UV radiations (312 nm) of **3aa**, **3ba**, **3da** and **3fa** in acetonitrile.

$\Phi_F = 0.90$) to 535 nm in diethyl ether (nonpolar solvent, Stokes shift = 10 000 cm^{-1}, $\Phi_F = 0.58$) (Table S9, SI). The blue shift of the emission spectra in polar solvents is attributed to the existence of the enol form in the excited state. Lippert's plot of compound **3fa** showed a linear correlation, confirming negative solvatochromism (Fig. S1, SI). The increase in fluorescence quantum yield with an increase in solvent polarity could be due to Intramolecular Charge Transfer (ICT).[22] Furthermore, to assess the selectivity towards different anions, fluorescence screening was carried out with compound **3aa** (Fig. 2).

In CH$_3$CN at 5×10^{-6} M, compound **3aa** interacted with 50 equivalents of various anions including Br$^-$, Cl$^-$, CN$^-$, F$^-$, I$^-$, HSO$_4^-$, NO$_3^-$, SCN$^-$, DCP, H$_2$PO$_4^-$ and HS$^-$. Strong fluorescence quenching and red shifts were observed with **3aa** for both F$^-$ and CN$^-$, while negligible changes occurred with other anions. The emission maxima of compound **3aa** were shifted to 570 nm for F$^-$ (25 nm shift) and 587 nm for CN$^-$ (62 nm shift) with fluorescence quenching. The fluorescence spectral titration of **3aa** with varying concentrations of F$^-$ and CN$^-$ anions in CH$_3$CN gave the limits of detection of 88 nM and 50 nM, respectively (Fig. S2 and S3, SI). The NMR titrations and Job's plots of **3aa** with F$^-$ and CN$^-$ ions indicated the interaction of the compound with ions through hydrogen bonds in a 1 : 2 ratio (Fig. S4–S8, SI).

In conclusion, we successfully developed a ruthenium-catalyzed C2 alkenylation of indoles using a cyclic amide of quinazolinone as a directing group. The reaction is compatible with a variety of substituents on the indole moiety and accommodates diverse alkenes. The alkenylated compounds demonstrated intriguing photophysical properties, including extended π-conjugation and negative solvatochromism. Additionally, compound **3aa** exhibited selective fluorescence-based detection of F$^-$ and CN$^-$ anions, establishing its potential as a fluorescent probe.
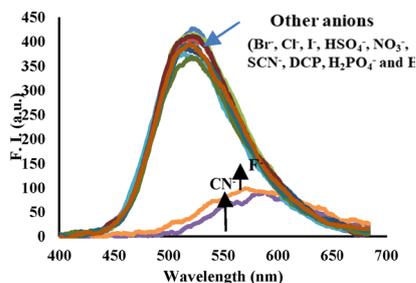

Fig. 2 Change in emission spectra of compound **3aa** (5 μM) with ions (250 μM).

Conflicts of interest

There are no conflicts to declare.

Data availability

The data supporting this article have been included as part of the SI. Supplementary information available: Experimental procedures, NMR, HRMS, and crystallographic data. See DOI: https://doi.org/10.1039/d5cc00984g

CCDC 2409835 contains the supplementary crystallographic data for this paper.[23]

Notes and references

1 T. V. Sravanthi and S. L. Manju, *Eur. J. Pharm. Sci.*, 2016, **91**, 1–10.
2 Y. Liu, K. Ai and L. Lu, *Chem. Rev.*, 2014, **114**, 5057–5115.
3 (a) N. Devi, K. Kaur, A. Biharee and V. Jaitak, *Curr. Med. Chem.: Anti-Cancer Agents*, 2021, **21**, 1802–1824; (b) P. V. Thanikachalam, R. K. Maurya, V. Garg and V. Monga, *Eur. J. Med. Chem.*, 2019, **180**, 562–612.
4 J. Kaur, D. Utreja, N. Jain and S. Sharma, *Curr. Organ. Synth.*, 2019, **16**, 17–37.
5 (a) C. A. Broka and J. A. Campbell, *US Pat.*, 6872744B2, 2005; (b) S. Singh, N. Sharma and R. Chandra, *Org. Chem. Front.*, 2022, **9**, 3624–3639.
6 S. S. Alharthi, *Chem. Pap.*, 2023, **77**, 7379–7394.
7 A. Kumari and R. K. Singh, *Bioorg. Chem.*, 2019, **89**, 103021.
8 (a) K. Urbina, D. Tresp, K. Sipps and M. Szostak, *Adv. Synth. Catal.*, 2021, **363**, 2723–2739; (b) P. Kumar, P. J. Nagtilak and M. Kapur, *New J. Chem.*, 2021, **45**, 13692–13746; (c) D. G. Matesanz, L. Gamarra, T. M. del Campo, P. Almendros and S. Cembellín, *ACS Catal.*, 2023, **13**, 14523–14529; (d) R. K. Shukla, A. Singh, R. Shetty and C. M. Volla, *Adv. Synth. Catal.*, 2025, **367**, e202401400; (e) C. Lázaro-Milla, J. L. Mascareñas and F. López, *ACS Catal.*, 2024, **14**, 2872–2882.
9 J. A. Leitch, Y. Bhonoah and C. G. Frost, *ACS Catal.*, 2017, **7**, 5618–5627.
10 (a) V. Lanke and K. R. Prabhu, *Chem. Commun.*, 2017, **53**, 5117–5120; (b) T. A. Shah, P. B. De, S. Pradhan and T. Punniyamurthy, *Chem. Commun.*, 2019, **55**, 572–587.
11 M. Mor, G. Spadoni, B. D. Giacomo, G. Diamantini, A. Bedini, G. Tarzia, P. V. Plazzi, S. Rivara, R. Nonno, V. Lucini and M. Pannacci, *Bioorg. Med. Chem.*, 2001, **9**, 1045–1057.
12 L. Kong, X. Zhou and X. Li, *Org. Lett.*, 2016, **18**, 6320–6323.
13 Y. Yang, P. Gao, Y. Zhao and Z. Shi, *Angew. Chem., Int. Ed.*, 2017, **56**, 3966–3971.
14 J. Lv, B. Wang, K. Yuan, Y. Wang and Y. Jia, *Org. Lett.*, 2017, **19**, 3664–3667.
15 (a) M. Y. Wong, T. Yamakawa and N. Yoshikai, *Org. Lett.*, 2015, **17**, 442–445; (b) K. Sakata, M. Eda, Y. Kitaoka, T. Yoshino and S. Matsunaga, *J. Org. Chem.*, 2017, **82**, 7379–7387; (c) J.-W. Li, S. Shi, M.-G. Huang, X.-H. Chen, L.-Y. Qiao and Y.-J. Liu, *J. Org. Chem.*, 2024, **90**, 35–43.
16 Z. Yang, J. Tang, C. Li, Z. Chen and X. F. Wu, *Chem. Commun.*, 2023, **59**, 318–321.
17 (a) R. Thakur and K. Paul, *J. Org. Chem.*, 2024, **89**, 6016–6026; (b) D. Singla, V. Luxami and K. Paul, *Eur. J. Org. Chem.*, 2023, e202300531.
18 W. Ma, K. Graczyk and L. Ackermann, *Org. Lett.*, 2012, **14**, 6318–6321.
19 R. Sharma and S. Chaudhary, *J. Org. Chem.*, 2022, **87**, 16188–16203.
20 Y. Zheng, W. B. Song, S. W. Zhang and L. J. Xuan, *Org. Biomol. Chem.*, 2015, **13**, 6474–6478.
21 H. Hazarika, D. Duttaa, S. Brahma, B. Das and P. Gogoi, *J. Org. Chem.*, 2022, **88**, 12168–12182.
22 S. Kothavale and N. Sekar, *ChemistrySelect*, 2017, **2**, 7691–7700.
23 R. Thakur, V. Luxami and K. Paul, CCDC 2409835: Experimental Crystal Structure Determination, 2025, DOI: 10.5517/ccdc.csd.cc2lwmmr.